

Atomic Structure of the Zr–He, Zr–vac, and Zr–vac–He Systems: First-Principles Calculation

O. V. Lopatina^{a,*}, Yu. M. Koroteev^b, and I. P. Chernov^a

^a National Research Tomsk Polytechnic University, pr. Lenina 30, Tomsk, 634050 Russia

^b Institute of Strength Physics and Materials Science, Siberian Branch, Russian Academy of Sciences, pr. Akademicheskii 2/4, Tomsk, 634021 Russia

* e-mail: lopatina_oksana@tpu.ru

Received May 18, 2016

Abstract—The ab initio investigations have been performed for the atomic structure of the Zr–He, Zr–vac, and Zr–vac–He systems with concentrations of helium atoms and vacancies (vac) of ~6 at %. A helium-induced instability of the zirconia lattice has been revealed in the Zr–He system, which disappears with the formation of vacancies. The most preferred positions of impurities in the metal lattice have been determined. The energy of helium dissolution and the excess volume introduced by helium have been calculated. It has been established that the presence of helium in the Zr lattice leads to a significant decrease in the energy of vacancy formation.

DOI: 10.1134/S1063783417010218

1. INTRODUCTION

Zirconium-based alloys are among the most important structural materials for fuel elements of pressurized water nuclear reactors [1]. During the operation of water nuclear reactors, these alloys accumulate helium impurity atoms formed in (n, α) nuclear reactions, as well as a large number of defects of both the thermodynamic and radiation origin. Owing to their low solubility in the metal, helium atoms are trapped by defects of the crystal lattice that contain excess volume regions, such as vacancies, dislocations, and grain boundaries. This leads to the formation of “lattice defect + helium” complexes, which are referred to in the literature as gas-filled bubbles [2–5]. In particular, the interaction of helium with vacancies in the metal results in the formation of vacancy complexes filled with helium [4, 5]. In [6, 7], it was reported that such helium bubbles can be formed at low temperatures with the participation of a single vacancy and a few helium atoms.

An increase in the concentration of vacancies in the material leads to an increase in the material volume. This phenomenon is called swelling. Furthermore, the accumulation of helium at the grain boundaries in polycrystals and the formation of vacancy complexes filled with helium in their volume cause the embrittlement of the material. These processes lead to the degradation of the performance properties of the structural materials [8–12]. The prevention of such undesirable phenomena requires a comprehensive investigation of the properties of the metal containing

point defects, such as vacancies and impurity atoms. Important information on the properties of the materials containing these defects can be obtained from first-principles calculations within the framework of the density functional theory.

The purpose of this study is to perform the ab initio investigations of the atomic structure of the Zr–He, Zr–vac, and Zr–vac–He systems with concentrations of impurity atoms and vacancies (vac) of ~6 at %. In particular, we have determined the most energetically favorable positions of the helium atoms in the lattice of a perfect Zr crystal and in the crystal with vacancies, calculated the energy of helium dissolution and the excess volume introduced by helium into the metal lattice, and investigated the influence exerted by the helium impurity on the energy of vacancy formation in zirconium.

2. COMPUTATIONAL METHOD AND DETAILS

The self-consistent calculations of the total crystal lattice energies of pure zirconium and the Zr–He, Zr–vac, and Zr–vac–He systems were carried out within the framework of the electron density functional theory in the generalized gradient approximation [13] using the linearized augmented plane-wave method [14, 15] implemented in the FLEUR program package [16]. The muffin-tin sphere radii of the Zr and He atoms were chosen to be equal to 2.3 and 1.0 a.u., respectively. The used value of the cutoff parameter of the plane-wave basis $k_{\max} = 4.0$ a.u.⁻¹ corresponded to

~170 basic functions per atom. In each self-consistent iteration, the eigenvalues of the Hamiltonian were calculated in 14 k -points of the Brillouin zone for the hexagonal close-packed (hcp) structures and in 10 k -points for the face-centered cubic (fcc) and body-centered cubic (bcc) structures. The self-consistent electron density calculation was performed until the convergence was no worse than 0.0001 meV/a.u.³, which corresponded to the convergence of the total crystal lattice energy of no worse than 0.001 meV. The optimization of the lattice parameters was carried out for all the systems under consideration. In addition, the relaxation of the crystal lattice of the metal near the vacancy was performed for the Zr–vac system.

The computational cell of the Zr–He system contained 16 metal atoms and one helium atom in the tetrahedral or octahedral interstitial site. The computational cells of the systems containing a vacancy (Zr–vac and Zr–vac–He) included 15 metal atoms and one vacant lattice site, whereas the computational cell of the Zr–vac–He system additionally contained one more helium atom in the tetrahedral or octahedral interstitial site near the vacancy or in the vacancy.

3. RESULTS AND DISCUSSION

3.1. Atomic Structure of the Zr–He System

In the first stage of our study, we investigated the stability of the fcc, bcc, and hcp zirconium lattices in the case where the concentration of dissolved helium atoms located in the tetrahedral or octahedral interstitial sites was equal to ~6 at %. The calculated dependences of the total crystal lattice energies E_{tot} of the Zr₁₆He system on the specific volume Ω per metal atom are shown in Fig. 1. It can be seen from this figure that the most energetically favorable structure is the hcp zirconium structure with a helium atom located in the octahedral interstitial site. In this case, the total energy $E_{\text{tot}}^{\text{hcp}}(\Omega)$ reaches (for the minimum specific volume $\Omega_{\text{min}} = 23.7 \text{ \AA}^3/\text{atom}$) the minimum value among all the structures considered for the Zr₁₆He system. However, we note that, in the octahedral coordination of the helium atom, the difference between the total energies of the hcp and fcc zirconium lattices with the specific volume $\Omega = \Omega_{\text{min}}$ does not exceed 2 meV/atom, whereas in the tetrahedral coordination of the impurity atom, the total energy $E_{\text{tot}}(\Omega_{\text{min}})$ for all the three considered crystal lattices exceeds the total energy $E_{\text{tot}}^{\text{hcp}}(\Omega_{\text{min}})$ by no more than 19 meV/atom. This means that all the crystal structures under consideration, except for the bcc lattice with the octahedral coordination of the helium atom, can be realized with an increase in the temperature to $T \sim 250 \text{ K}$ (in this case, the difference between the total energies is 21 meV/atom), whereas at operating temperatures of nuclear reactor fuel elements (350–400°C), all the structures considered in our study can

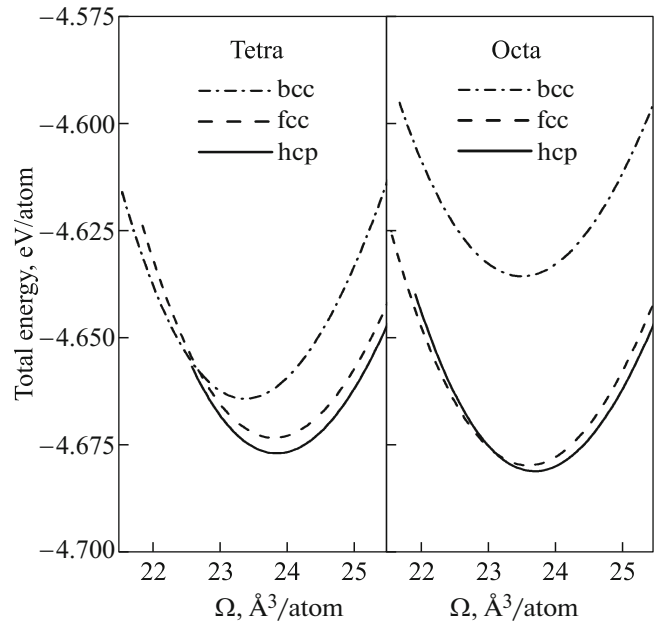


Fig. 1. Dependences of the total crystal lattice energy of the Zr–He system on the specific volume Ω per metal atom of the hcp, fcc, and bcc lattices for the tetrahedral and octahedral coordinations of the helium atom. The energy is measured from the total energy of the hcp structure of pure zirconium.

be realized. It should also be noted that the hydrostatic compression (the transition to the range of specific volumes $\Omega < \Omega_{\text{min}}$) leads to the coexistence of these structures also at lower temperatures. Thus, it is found that, at a helium concentration of ~6 at %, the crystal structure of zirconium exhibits an instability both with an increase in the temperature and under hydrostatic pressure.

This behavior of the system can be understood by analyzing the results obtained in our earlier work [17], where we investigated the stability of the crystal lattice of the Zr–He system at a higher helium concentration as compared to that considered in the present study. In [17], we also calculated the dependences $E_{\text{tot}}(\Omega)$ for different crystal lattices of pure zirconium and the Zr–He system. By comparing the results obtained in the present study with the data reported in [17], we can conclude that the location of a helium atom in the zirconium lattice, in some sense, is equivalent to a compression of the crystal. Indeed, the higher helium concentration considered in [17] stabilizes the bcc zirconium lattice, which is realized in the pure metal only under pressure, i.e., with a decrease in the specific volume of the metal from the equilibrium value $\Omega_{\text{min}} = 23.27 \text{ \AA}^3/\text{atom}$ to the value of $\sim 18.5 \text{ \AA}^3/\text{atom}$ [17, Fig. 1]. The lower helium concentration (~6 at %) considered in the present study probably correspond to lower pressures in pure zirconium and, therefore, to higher values of the specific volume Ω as compared to

Table 1. Energy of helium dissolution in zirconium

Lattice type	ΔE , eV			
	Tetrahedral interstitial site		Octahedral interstitial site	
	this work	[17]	this work	[17]
hcp	3.67	3.08	3.61	3.19
fcc	3.37	3.09	3.28	3.28
bcc	2.84	2.63	3.25	3.02

the previous case. In particular, according to the data presented in [17, Fig. 1], for pure zirconium in the range of specific volumes $\Omega \sim 19.3 \text{ \AA}^3/\text{atom}$, the functional dependences $E_{\text{tot}}(\Omega)$ of all the crystal structures under consideration come very close to each other and intersect. This indicates that the crystal lattice of the metal is characterized by the instability at pressures corresponding to the aforementioned specific volume.

As is known, the presence of impurity atoms in a crystal leads to an increase in the crystal volume. In the present study, we calculated the values of the excess volume $\Delta\Omega$ introduced by the helium atom into the fcc, bcc, and hcp zirconium lattices, which was determined as the difference between the volume of the crystal with helium impurity atoms and the volume of the pure crystal. The calculations demonstrated that the smallest excess volume is introduced by helium atoms into the hcp lattice and that the minimum value of this volume $\Delta\Omega \sim 6.2 \text{ \AA}^3/\text{atom}$ corresponds to the octahedral coordination of the helium atoms. This correlates with the conclusion that the most energetically favorable structure is the hcp zirconium structure. The latter is most likely associated with the fact that the size of the tetrahedral interstitial sites in the crystal lattices under consideration is almost two times smaller than the size of the octahedral interstitial sites.

The energy of helium dissolution in zirconium was calculated according to the formula

$$\Delta E = E_{\text{tot}}(\text{Zr}_n\text{He}) - E_{\text{tot}}(\text{Zr}_n) - E_{\text{tot}}(\text{He}), \quad (1)$$

where $E_{\text{tot}}(\text{Zr}_n\text{He})$, $E_{\text{tot}}(\text{Zr}_n)$, and $E_{\text{tot}}(\text{He})$ are the total energies of the Zr_nHe system, pure zirconium, and an isolated helium atom, respectively, and n is the number of zirconium atoms in the computational cell (in this case, $n = 16$). For the total energy $E_{\text{tot}}(\text{He})$, we used the value of -78.5044 eV obtained in our self-consistent calculation of a single helium atom.

The calculated energies of helium dissolution in zirconium are presented in Table 1. As can be seen from this table, the energy of helium dissolution has positive values for all the three crystal structures under consideration. This suggests that, under normal conditions, helium does not dissolve in zirconium and can penetrate into the bulk of the material only under specific conditions, for example, during the implantation of helium ions into the metal or as a result of the (n, α) nuclear reactions occurring in the material under irra-

diation with neutrons. The minimum and maximum energies of helium dissolution in zirconium correspond to the bcc and hcp zirconium lattices, respectively. Moreover, in the case of the bcc zirconium lattice, the energy of helium dissolution in tetrahedral interstitial sites is less than that in octahedral interstitial sites, whereas the opposite situation is observed in the fcc and hcp structures of zirconium. For comparison, Table 1 also presents the results obtained from the calculations of the energies of helium dissolution in zirconium at a higher impurity concentration [17]. It can be seen that, at the higher concentration of helium impurity atoms, the energies of helium dissolution in interstitial sites of all the crystal lattices under consideration are less than the corresponding values at the helium concentration of $\sim 6 \text{ at } \%$ by $0.2\text{--}0.6 \text{ eV}$, with the exception of the octahedral interstitial sites of the fcc lattice, where the dissolution energy remains almost unchanged. A similar dependence of the energy of impurity dissolution on the impurity concentration was observed in [18] for bcc transition metals Fe, Cr, and Mo at lower helium concentrations (~ 0.8 and $\sim 1.8 \text{ at } \%$), where the decrease in the dissolution energy was of the order of $0.06\text{--}0.18 \text{ eV}$. The relatively small change in the dissolution energy in this case is associated with the fact that the aforementioned concentrations are close to each other. This functional dependence of the energy of helium dissolution in the metal on the helium concentration apparently is determined by the significant increase in the lattice parameters of the crystal with an increase in the helium concentration under conditions of a very weak chemical interaction between helium and zirconium.

3.2. Atomic Structure of the Zr–vac System

In this study, we also investigated the atomic structure of the Zr–vac system. The dependences of the total crystal lattice energy of the Zr–vac system on the specific volume per lattice (including vacant) site are shown in Fig. 2. It can be seen from this figure that the most energetically favorable structure is the hcp structure of the metal, because the total energy in this case reaches the minimum value among all the structures considered for the Zr–vac system. The equilibrium specific volumes Ω_v for the hcp, fcc, and bcc struc-

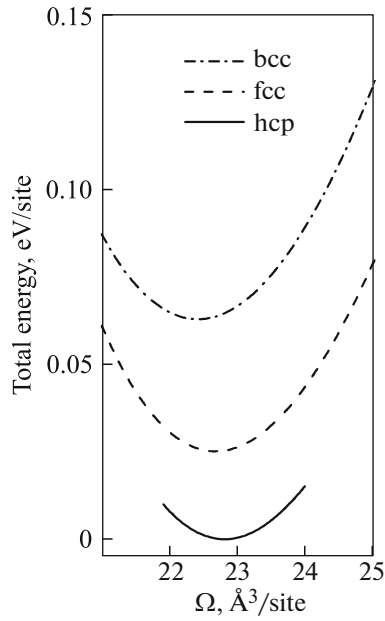


Fig. 2. Dependences of the total energy of the Zr–vac system on the specific volume Ω per lattice (including vacant) site of the hcp, fcc, and bcc structures. The energy is measured from the total energy of the hcp structure of the Zr–vac system.

tures are equal to 22.85, 22.74, and 22.36 $\text{\AA}^3/\text{site}$, respectively. The values of the equilibrium specific volume Ω of pure zirconium without vacancies for the same structures are equal to 23.26, 23.06, and 22.77 $\text{\AA}^3/\text{site}$, respectively. Thus, the presence of ~ 6 at % vacancies in zirconium leads to a decrease in the equilibrium specific volume of the sample by 1.4–1.8%. These values are in good agreement with the experi-

mental data obtained in [19] and, qualitatively, with the results of the ab initio calculation using the Green's function method [20].

The energies of vacancy formation E_v in the hcp, fcc, and bcc zirconium lattices were calculated according to the formula

$$E_v = E_{\text{tot}}(\text{Zr}_{n-1}) - E_{\text{tot}}(\text{Zr}_n)(n-1)/n, \quad (2)$$

where $E_{\text{tot}}(\text{Zr}_n)$ is the total energy of the perfect zirconium crystal (here, n is the number of atoms in the computational cell) and $E_{\text{tot}}(\text{Zr}_{n-1})$ is the total energy of the zirconium crystal with a vacancy. The calculated energies of vacancy formation E_v in different crystallographic modifications of zirconium (with the inclusion of the relaxation of the crystal lattice and without it), as well as the results obtained in the calculations of other authors [20–28] and the corresponding experimental data [29], for the three crystal structures under consideration, are presented in Table 2. According to our calculations taking into account the relaxation of the crystal lattice, the minimum and maximum energies of vacancy formation are observed in the bcc and fcc zirconium lattices, respectively. In the first case, the minimum energy of vacancy formation apparently is caused by the lowest (among the structures under consideration) degree of close packing of zirconium atoms in the bcc crystal, where each atom has eight nearest neighbors, whereas in the fcc and hcp crystal lattices, each zirconium atom has 12 nearest neighbors. This also explains the most significant influence of the relaxation on the vacancy formation energy E_v in the bcc zirconium lattice, which manifests itself in a decrease of this energy by 0.77 eV (as compared to 0.05 and 0.11 eV in the fcc and hcp crystals, respectively). In the second case, the maximum energy of vacancy formation apparently is asso-

Table 2. Energy of vacancy formation E_v in different crystallographic modifications of zirconium

Lattice type	E_v , eV			
	this work		calculations of other authors	experiment
	without the inclusion of the relaxation	with the inclusion of the relaxation		
fcc	2.23	2.18	1.77 [20]	1.70 [29]
bcc	2.18	1.41	1.68 [20] 2.34, 2.30 [28]	
hcp	2.15	2.04	1.86 [21] 1.75 [22] 1.79 [23] 1.74 [24] 1.93, 2.07 [25] 1.55 [26] 1.70, 1.86 [27] 2.07 [28]	

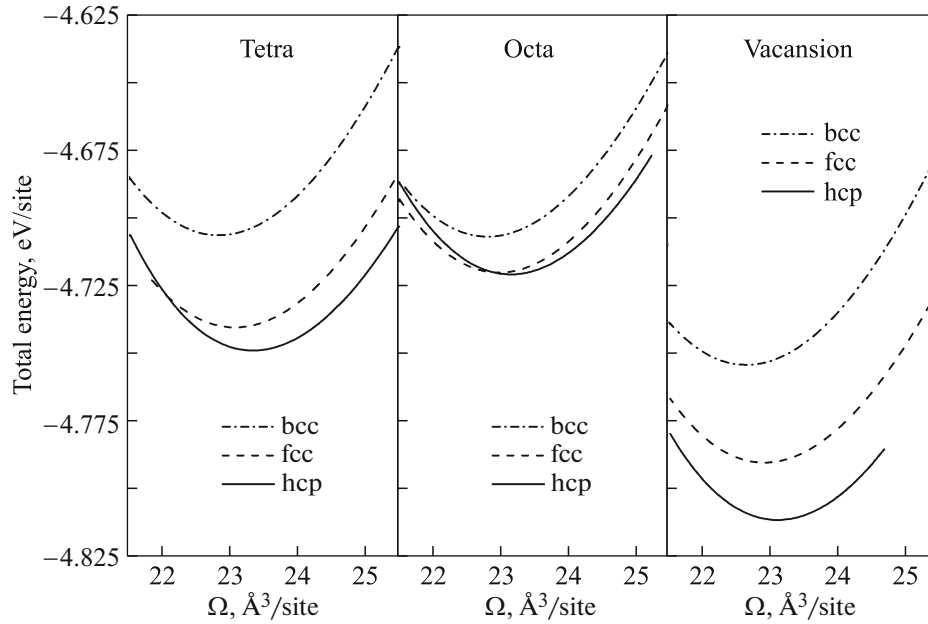


Fig. 3. Dependences of the total energy of the Zr–vac–He system on the specific volume Ω per lattice (including vacant) site of the hcp, fcc, and bcc structures for the tetrahedral and octahedral coordinations of the helium atom, as well as for the He atom in a vacancy. As in Fig. 2, the energy is measured from the total energy of the hcp structure of the Zr–vac system.

ciated with the fact that the distance between the nearest neighbors in the fcc zirconium lattice (2.26 Å) is significantly shorter than that in the hcp zirconium crystal (2.58 and 3.22 Å), and, consequently, the binding forces between the atoms in the fcc zirconium lattice are stronger than those in the hcp zirconium lattice.

The energy of vacancy formation in the hcp zirconium lattice, which was calculated in [21–28], varies in the range from 1.55 to 2.07 eV. This spread of the values can be explained by the use of a number of methods (ab initio or semi-empirical) and calculation conditions (with the inclusion of the relaxation and without it), as well as by different concentrations of vacancies. The value of E_v obtained in our calculation is within this spread and agrees satisfactorily with the experimental data. The vacancy formation energies found by us for the fcc and bcc zirconium lattices are in reasonable agreement with the results obtained in the calculations of other authors.

3.3. Atomic Structure of the Zr–Vac–He System

The calculated dependences of the total energy of the Zr–vac–He system on the specific volume per lattice (including vacant) site for the three crystal structures under consideration are shown in Fig. 3. For each of these structures, we analyzed three variants of the location of the helium atoms in the metal lattice: (i) tetrahedral interstitial site of the first coordination sphere of the vacancy, (ii) octahedral interstitial site of the first coordination sphere of the vacancy, and

(iii) vacancy. It can be seen from Fig. 3 that the most energetically favorable position of the helium atom in all the crystal lattices under investigation is the vacancy. For all three variants of the arrangement of the helium atoms, the most energetically favorable structure is the hcp zirconium lattice. It is interesting to note that, in the immediate vicinity of the vacancy, the octahedral interstitial site, which is energetically more favorable for helium in the Zr–He system (Fig. 1), becomes energetically less favorable with respect to the tetrahedral interstitial site in the Zr–vac–He system.

Table 3 presents the energies of helium dissolution in the Zr–vac system for the three crystal structures under consideration, which were calculated according to the formula

$$\Delta E_v = E_{\text{tot}}(\text{Zr}_{n-1}\text{He}) - E_{\text{tot}}(\text{Zr}_{n-1}) - E_{\text{tot}}(\text{He}), \quad (3)$$

Table 3. Energy of helium dissolution in the tetrahedral and octahedral interstitial sites of the Zr–vac system near the vacancy and in the vacancy

Lattice type	ΔE_v , eV		
	vacancy	tetrahedral interstitial site	octahedral interstitial site
hcp	1.51	2.51	2.97
fcc	1.49	2.27	2.60
bcc	1.42	2.18	2.20

Table 4. Energy of vacancy formation $E_v(\text{Zr-He})$ in different crystallographic modifications of the Zr-He system

Lattice type	$E_v(\text{Zr-He}), \text{eV}$	
	tetrahedral interstitial site	octahedral interstitial site
fcc	1.09	1.57
bcc	1.53	1.11
hcp	1.06	1.56

where $E_{\text{tot}}(\text{Zr}_{n-1}\text{He})$, $E_{\text{tot}}\text{Zr}_{n-1}$, and $E_{\text{tot}}(\text{He})$ are the total energies of the Zr-vac-He system, the Zr-vac system, and an isolated helium atom, respectively. As can be seen from Table 3, the energy of helium dissolution in the Zr-vac system has positive values for all the three crystal lattices under consideration. In each of these lattices, the energy of helium dissolution in the system has the minimum value in the case where the helium atom is located in the vacant site of the zirconium crystal.

A comparison of the data presented in Tables 1 and 3 demonstrates that, in the presence of vacancies in zirconium, the energy of helium dissolution in tetrahedral interstitial sites of the hcp and fcc zirconium lattices and in octahedral interstitial sites of the bcc zirconium lattice decreases by ~ 1.1 eV. In this case, the energy of helium dissolution in octahedral interstitial sites of the hcp and fcc lattices and in tetrahedral interstitial sites of the bcc structure decreases by ~ 0.67 eV. Apparently, this is associated with the fact that the Zr-vac system is as if under a negative pressure, because the presence of vacancies in the metal leads to a decrease in the equilibrium specific volume of the sample, as was noted in Subsection 3.2. In this case, the excess volume introduced by helium upon the dissolution in the Zr-vac system is effectively reduced, which leads to a decrease in the dissolution energy.

We are not aware of papers devoted to the investigation of vacancy-helium complexes in zirconium. Therefore, we compared our results with the data obtained from theoretical studies on the energetics of matrix-vacancy-helium systems, where the role of the matrix was played by the bcc (α -Fe, Cr, Mo, W, V, Nb, Ta) [6, 18, 30], fcc (Ni, Cu, Ag, Pd) [18], and hcp (Er, Sc, Y, Gd, Tb, Dy, Ho, Lu) [31–33] metals. The energies of helium dissolution in the crystal with vacancies, which were calculated in the aforementioned works, have positive values, as in our case for zirconium. For all the crystal structures under consideration, the minimum energy of helium dissolution corresponds to the situation where the helium atom is located in the vacancy. In this case, the energy of helium dissolution in tetrahedral interstitial sites is less than that in octahedral interstitial sites. All this is consistent with the results of the present study.

We also calculated the energy of vacancy formation in the Zr-He system for the three crystal structures under consideration according to the formula

$$E_v(\text{Zr-He}) = E_{\text{tot}}(\text{Zr}_{n-1}\text{He}) - E_{\text{tot}}(\text{Zr}_n\text{He}) + v/nE_{\text{tot}}(\text{Zr}_n), \quad (4)$$

where $E_{\text{tot}}(\text{Zr}_{n-1}\text{He})$ and $E_{\text{tot}}(\text{Zr}_n\text{He})$ are the total energies of the Zr-He systems in the presence of a vacancy and without it, respectively, and v is number of vacancies in the computational cell (in this case, $v = 1$). The calculated energies of vacancy formation $E_v(\text{Zr-He})$ in different crystallographic modifications of the Zr-He system are presented in Table 4. A comparison of these results with the data obtained for the defect-free pure metal (see the vacancy formation energies without the inclusion of the relaxation in Table 2) demonstrates that the presence of helium in zirconium decreases the energy of vacancy formation in all the systems studied in the present work. Since the Zr-He and Zr-vac-He systems were considered without taking into account the relaxation of the crystal lattice of the metal in the vicinity of defects, the energies of vacancy formation in the Zr-He system were compared with the corresponding (unrelaxed) values for the pure metal.

4. CONCLUSIONS

In this work, we carried out the ab initio investigations of the atomic structure of the Zr-He, Zr-vac, and Zr-vac-He systems with concentrations of helium atoms and vacancies of ~ 6 at % for the hcp, fcc, and bcc lattices of the metal. The calculations of the total energies of these systems demonstrated that the presence of helium with a concentration of ~ 6 at % in the Zr-He system gives rise to an instability of the hcp zirconium lattice, where the formation of vacancies in this system, on the contrary, results in the stabilization of the zirconium lattice. The most preferred positions of the helium atom in the Zr-vac-He system are vacancies, the presence of which decreases the energy of helium dissolution in zirconium. It was found that the presence of helium in the zirconium lattice leads to a significant decrease in the energy of vacancy formation.

REFERENCES

1. A. S. Zaimovskii, A. V. Nikulina, and N. G. Reshetnikov, *Zirconium Alloys in Atomic Power Engineering* (Energoatomizdat, Moscow, 1981) [in Russian].
2. Y. Ishiyama, M. Kodama, N. Yokota, K. Asano, T. Kato, and K. Fukuya, *J. Nucl. Mater.* **239**, 90 (1996).
3. R. E. Stoller and G. R. Odette, *J. Nucl. Mater.* **154**, 286 (1988).
4. M. B. Lewis and K. Farrell, *Nucl. Instrum. Methods Phys. Res., Sect. B* **16**, 163 (1986).

5. R. Vassen, H. Trinkaus, and P. Jung, *Phys. Rev. B: Condens. Matter* **44** (9), 4206 (1991).
6. C.-C. Fu and F. Willaime, *Phys. Rev. B: Condens. Matter* **72** (6), 064117, (2005).
7. G. Thomas and R. Bastasz, *J. Appl. Phys.* **52** (10), 6426 (1981).
8. V. F. Zelenskii, I. M. Neklyudov, and T. P. Chernyaeva, *Radiation Defects and Swelling of Metals* (Naukova Dumka, Kiev, 1988) [in Russian].
9. *Fundamental Aspect of Inert Gases in Solids*, Ed. by S. E. Donnelly and J. H. Evans (Plenum, New York, 1991).
10. T. Ishizaki, Q. Xu, T. Yoshiie, S. Nagata, and T. Troev, *J. Nucl. Mater.* **307–311**, 961 (2002).
11. H. Trinkaus and B. N. Singh, *J. Nucl. Mater.* **323**, 229 (2003).
12. I. M. Neklyudov and G. D. Tolstolutskaia, *Vopr. At. Nauki Tekh., Ser.: Fiz. Radiats. Povrezhdenii Radiats. Materialoved.*, No. 3, 3 (2003).
13. J. P. Perdew, K. Burke, and M. Ernzerhof, *Phys. Rev. Lett.* **77** (18), 3865 (1996).
14. E. Wimmer, H. Krakauer, M. Wienert, and A. J. Freeman, *Phys. Rev. B: Condens. Matter* **24** (2), 864 (1981).
15. M. Wienert, E. Wimmer, and A. J. Freeman, *Phys. Rev. B: Condens. Matter* **26** (8), 4571 (1982).
16. <http://www.flapw.de>
17. Yu. M. Koroteev, O. V. Lopatina, and I. P. Chernov, *Phys. Solid State* **51** (8), 1600 (2009).
18. X. T. Zu, L. Yang, F. Gao, S. M. Peng, H. L. Heinisch, X. G. Long, and R. J. Kurtz, *Phys. Rev. B: Condens. Matter* **80** (5), 054104 (2009).
19. P. Ehrhart, P. Jung, H. Schultz, and H. Ullmaier, in *Atomic Defects in Metals*, Landolt–Börnstein, New Series, Group III/25, Ed. by H. Ullmaier (Springer-Verlag, Berlin, 1991).
20. P. A. Korzhavyi, I. A. Abrikosov, B. Johansson, A. V. Ruban, and H. L. Skriver, *Phys. Rev. B: Condens. Matter* **59** (18), 11693 (1999).
21. C. Domain and A. Legris, *Philos. Mag.* **85**, 569 (2005).
22. Y. Dai, J. H. Li, and B. X. Liu, *J. Phys.: Condens. Matter* **21**, 385402 (2009).
23. G. J. Ackland, *Philos. Mag. A* **66**, 917 (1992).
24. R. C. Pasianot and A. M. Monti, *J. Nucl. Mater.* **264**, 198 (1999).
25. M. I. Baskes and R. A. Johnson, *Modell. Simul. Mater. Sci. Eng.* **2**, 147 (1994).
26. M. Fuse, *J. Nucl. Mater.* **136**, 250 (1985).
27. D. J. Oh and R. A. Johnson, *J. Nucl. Mater.* **169**, 5 (1989).
28. O. Le Bacq, F. Willaime, and A. Pasturel, *Phys. Rev. B: Condens. Matter* **59** (13), 8508 (1999).
29. F. R. de Boer, R. Boom, W. C. M. Matters, A. R. Miedema, and A. K. Niessen, *Cohesion in Metals: Transition Metal Alloys* (North-Holland, Amsterdam, 1988).
30. T. Seletskaiia, Y. Osetsky, R. E. Stoller, and G. M. Stocks, *Phys. Rev. Lett.* **94** (4), 046403 (2005).
31. L. Yang, S. M. Peng, X. G. Long, F. Gao, H. L. Heinisch, R. J. Kurtz, and X. T. Zu, *J. Appl. Phys.* **107** (5), 054903 (2010).
32. L. Yang, S. M. Peng, X. G. Long, F. Gao, H. L. Heinisch, R. J. Kurtz, and X. T. Zu, *J. Phys.: Condens. Matter* **23**, 035701 (2011).
33. L. Yang, R. C. Chen, S. M. Peng, X. G. Long, Z. C. Wu, F. Gao, and X. T. Zu, *Sci. China Phys., Mech. Astron.* **54**, 827 (2011).

Translated by O. Borovik-Romanova